M- and L-shell ionization in near-central collisions of 5.5-MeV/amu ^{16}O ions with Mo atoms deduced from theoretical analysis of high-resolution K x-ray spectra

M. W. Carlen, M. Polasik,* B. Boschung, J.-Cl. Dousse, M. Gasser, Z. Halabuka, J. Hoszowska, J. Kern, B. Perny, and Ch. Rhême
Physics Department, University of Fribourg, CH-1700 Fribourg, Switzerland

P. Rymuza† and Z. Sujkowski
Institute for Nuclear Studies, 05-400 Świerk, Poland
(Received 13 April 1992)

The $K\alpha$ and $K\beta$ x-ray spectra of molybdenum bombarded by 5.5-MeV/amu ^{16}O ions were measured with high resolution. In such heavy-ion–atom collisions, multiple ionization of the M and L shells of the target atoms is extremely likely to occur, resulting in a complex structure of the observed spectra. The L^n-satellite structure was resolved, whereas M vacancies produce only a shift and a broadening of the lines so that it is not possible to obtain in a direct way information about the M-hole distribution. We thus propose a method for the analysis of x-ray spectra of multiply ionized atoms. In this method the measured $K\alpha$ and $K\beta$ spectra are simultaneously analyzed as a sum of $K\alpha L^n M^m$ and $K\beta L^n M^m$ components, respectively, with theoretically determined profiles. A binomial distribution of holes in the M shell is assumed and the M-shell ionization probabilities are treated as adjustable parameters. The profiles are constructed as sums of Voigt functions, whose positions and heights are determined by extensive multiconfiguration Dirac-Fock method calculations. If, in a simultaneous fit to the $K\alpha L^0$ and $K\beta_{1,3}L^0$ lines, just one parameter p_M^X describing the M-shell ionization at the moment of the K x-ray transition is used, the experimental data are not reproduced in an entirely satisfactory way ($p_M^X=0.19\pm0.02$). Therefore, two parameters, one common for the $3s$ and $3p$ subshells p_{3sp}^X and the other for the $3d$ subshells, were introduced and a much better fit to both lines ($p_{3sp}^X=0.17\pm0.02$, $p_{3d}^X=0.23\pm0.02$) was obtained. The importance and influence of alternative ionizing processes as electron-capture and rearrangement processes are discussed and the M-shell ionization probability at the moment of the collision ($p_M=0.18\pm0.02$) is deduced from the p_M^X value. It is shown that the differences between p_{3sp}^X and p_{3d}^X are mainly due to Coster-Kronig transitions, rather than due to different subshell ionization probabilities. The spectra were also analyzed with respect to the L-shell ionization on the basis of the calculated $K\alpha L^n M^0$, $K\beta_{1,3}L^n M^0$, and $K\beta_2 L^n M^0$ components. The M-shell ionization was taken into account by taking a larger Gaussian width and by shifting the positions of the lines. The intensity yields of the L satellites were determined, the primary vacancy distribution was deduced, and the results from $K\alpha$ and $K\beta$ spectra are compared.

PACS number(s): 32.30.Rj, 32.70.Jz, 34.50.Fa, 35.80.+s

I. INTRODUCTION

It is well established that in a collision of an energetic heavy ion with an atom, multiple ionization of the inner shells plays an important role. For the ionized atom many different configurations are possible, depending on the number of electrons ejected from the different shells and subshells. A particular configuration with more than one open subshell gives rise to many configuration-state functions, which may differ in their total angular momentum J.

The excited atom decays by filling up the inner-shell holes via x-ray or Auger transitions. For a particular configuration dozens or hundreds of initial and final states may exist and between these states hundreds or thousands of transitions (with different energies) are possible. Therefore, a measured x-ray line may consist of many thousand components and has a very complex structure.

X-ray transitions between multiply ionized states are called satellite transitions. Since the removal of electrons modifies the screening of the nuclear charge, the x-ray satellites are shifted in energy with respect to the energy of the diagram transition. The energy shifts for satellite x-ray transitions increase on one hand with the principal quantum number characterizing the electron undergoing the transition and decrease on the other hand with the principal quantum number of a spectator vacancy. Therefore, a $K\beta L^1$ satellite, i.e., a $K\beta$ transition with one additional hole in the L shell, is more shifted in energy than a $K\alpha L^1$ satellite, while a $K\alpha L^1$ satellite is more shifted than a $K\alpha M^1$ one.

Measuring the K x-ray spectra of medium-Z elements with high-resolution instruments, it is possible to resolve the L satellites for $K\beta$ and $K\alpha$ transitions. On the contrary, energy shifts induced by additional M-shell vacancies are in general smaller than the natural linewidths of the diagram and L-satellite K x-ray lines. The latter are therefore just broadened and shifted by the removal of M-shell electrons. The $K\beta_2$ transition is, however, a re-

markable and stirring exception: due to the fact that the transition electron comes from the N shell, the energy shift is much larger and in that case $K\beta_2 M^m$ satellites may be observed as well-resolved lines, for example, in spectra induced by He beams [1,2].

In the beginning of the 1970s a method was developed to determine the L-shell ionization probability in near-central collisions from measured K x-ray spectra. This method has been applied to many studies of target elements with Z smaller than 30 [3–25]. From 1987 on, target elements with $Z \geq 40$ have also been investigated [26–31]. Carlen *et al.* [1,2] extended this method to determine the M-shell ionization probability in near-central collisions with light ions as projectiles.

There are several advantages in measuring K x rays instead of L or M x rays for the study of the L- or M-shell ionization process.

(i) The ionization probabilities determined by this method are valid for near-central collisions, i.e., they represent values valid for a narrow impact-parameter range. This is of special interest since, with the total cross sections due to an integration over the whole impact-parameter range resulting in smearing out of oscillation effects, a detailed comparison with the theoretical predictions cannot always be made. Furthermore, a direct measurement of the differential cross section is connected with experimental difficulties, especially for the M shell.

(ii) To determine the ionization cross section from observed x-ray yields, the knowledge of the Auger and Coster-Kronig yields is necessary, which have large uncertainties. In the analysis of K x rays, these quantities only enter in the rearrangement calculation, which is a correction for processes occurring before the ionized atom emits the K x ray. This correction is rather small since the decay of the K hole is very fast, so that the configuration of the atom at the moment of the K x-ray transition is not very different from its configuration after the collision.

(iii) Since the K x rays are of higher energy, the spectra are much less complicated than L or M x-ray spectra and target contaminations from low-Z elements have no effect.

We have performed high-resolution measurements of the $K\alpha$ and $K\beta$ x-ray spectra of $_{42}$Mo bombarded by 5.5-MeV/amu ^{16}O ions. The measured $K\alpha$ spectrum was presented in Ref. [26]. Rymuza *et al.* [27] found from the analysis of the $K\alpha L^n$ satellite distribution that, besides direct Coulomb ionization, electron capture to the projectile must play an important role in the ionization process. Polasik [32–34] performed theoretical calculations using the multiconfiguration Dirac-Fock (MCDF) program of Grant *et al.* [35] and compared the theoretical $K\alpha L^n$ spectrum with the measured one. He concluded that, due to the complexity of the experimental $K\alpha$ x-ray spectra of multiply ionized atoms, a correct analysis needs theoretical knowledge of the structure of $K\alpha L^n$ lines and the effect of M-shell holes has to be taken into account. The present method has been therefore developed to determine the distribution of M-shell holes at the moment of the x-ray emission.

In this paper we concentrate on the determination of the M-shell hole distribution by analyzing the $K\alpha L^0$ and $K\beta_{1,3}L^0$ lines. The obtained result is compared with one from semiclassical-approximation (SCA) calculations. Furthermore, the L-shell hole distribution is determined from the $K\alpha L^n$ and $K\beta_{1,3}L^n$ lines and the results from $K\alpha$ and $K\beta$ are compared.

II. EXPERIMENT

The experiments were performed at the Paul Scherrer Institute variable-energy cyclotron in Villigen, Switzerland. The x rays, produced by a 5.5-MeV/amu ^{16}O ion beam impinging on a natural molybdenum target, were measured with an in-beam bent crystal spectrometer in a modified DuMond slit geometry. The experimental setup has been described in detail elsewhere [36] and the advantages of the slit geometry have been pointed out in Ref. [2]. Figures 1(a) and 1(b) show the oxygen-induced $K\alpha$ and $K\beta$ x-ray spectra. Figures 1(c) and 1(d) show for comparison the corresponding photoinduced spectra which have been taken with a 3-kW x-ray tube operated at 80 kV and equipped with an Au anode.

$^{16}O^{4+}$ ions were accelerated by the cyclotron to an energy of 112 MeV. Beam intensities of about 100 nA were used. The ions were fully stripped by passing the 4.4-mg/cm^2 Havar entrance window in the target chamber. The 11-mg/cm^2-thick self-supported metallic target foil was cooled by a He gas flow, pumped through the target chamber. Taking into account the energy loss in the Havar foil, self-absorption and stopping power of the target, and the energy dependence of the K-shell ionization cross section, the effective beam energy for producing the observed x rays was about 5.5 MeV/nucleon.

Quartz crystal plates of 1.5-mm and 2.5-mm thickness and dimensions 10×10 cm^2, clamped between two steel

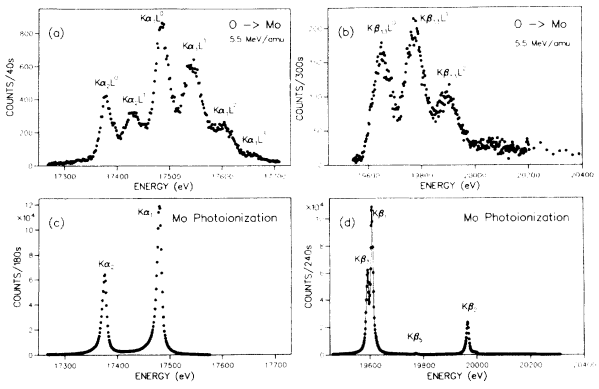

FIG. 1. High-resolution crystal spectrometer spectra of molybdenum K x rays. (a) 5.5-MeV/amu ^{16}O-induced $K\alpha$ spectrum. (b) 5.5-MeV/amu ^{16}O-induced $K\beta$ spectrum. (The correction for the increased self-absorption for energies higher than the K-edge energy is not taken into account.) (c) Photoinduced $K\alpha$ x-ray spectrum. (d) Photoinduced $K\beta$ x-ray spectrum.

blocks, have been used. The blocks have cylindrical surfaces with a radius of curvature of 3.15 m. The reflecting planes were the (110) planes and the reflecting area was 5×5 cm^2. The peak reflectivity of the crystals was enhanced by a factor of 3–4 by applying a high-frequency alternating electric field across the lamina [37]. This field produces periodic deformations of the reflecting planes resulting in an induced quasimosaicity of the crystal which increases its reflectivity. The deterioration of the resolution is negligible with respect to the large natural linewidths of the x rays.

The instrumental resolution and the line shape were obtained by measuring the 25.7-keV γ-ray line in the ^{161}Tb decay. They mainly depend on the slit width, the crystal mosaicity and curvature, and on the ac voltage applied to the crystal. The radioactive source was placed 30 cm behind the target and was observed through the slit. The instrumental resolution was chosen to match the natural linewidth of the K diagram lines. According to Salem and Lee [38] the Lorentzian width of the $K\alpha_1$ transition of Mo is 6.8 eV and an extrapolation of these tables gives for the $K\beta_1$ transition a natural linewidth of about 6.5 eV. The full width at half maximum (FWHM) of the Gaussian function, representing the instrumental line shape, was 6.5 eV at 17.4 keV ($K\alpha$) and 8.0 eV at 19.6 keV ($K\beta$).

A 1-mm-thick NaI(Tl) detector, surrounded by an anti-Compton ring was used. The beam intensity was monitored by observing the target $K\alpha$ x rays with a 6-cm^3 Ge(Li) detector positioned at 90° with respect to the beam line. The spectra were measured in first order of reflection and in several scannings, in order to survey the stability and reproducibility of the measurements. The energy calibration is based on the 48.915 62(14)-keV γ line [39] in the ^{161}Tb decay, measured in the second and third order on both sides of reflection. The reflection angles were measured by means of an optical laser interferometer.

As a result of the shift towards higher energies of the satellite transitions relating to the diagram ones, a part of the measured $K\beta$ spectrum lies above the K edge, which is at 19.9995 keV for Mo [40]. For this part of the spectrum the self-absorption in the target is strongly increased. Taking into account the dependence of the ionization cross section on the projectile energy, the measured intensities of this region of the spectrum were multiplied by a factor of 1.5(2), after subtraction of the background.

III. METHOD OF ANALYSIS

In order to illustrate the complexity of the Mo K x-ray spectra induced by oxygen ions, a comparison with the photoinduced one is presented in Fig. 1. The conspicuous differences are due to the fact that, in the case of the collisions with energetic O ions the M and L shells of the Mo atom are multiply ionized. For example, in the O-induced spectrum the $K\beta_1$ and $K\beta_3$ lines are not resolved and form just one broad peak $K\beta_{1,3}L^0$. Also the $K\beta_2$ transition is not resolved but disappears in a broad and flat bump. However, the $K\beta_{1,3}L^1$ and $K\beta_{1,3}L^2$ satellite lines have high intensity and can be recognized. From the relative intensities of the L satellites we can get the distribution of holes in the L shell at the moment of the x-ray transition. On the contrary, additional M-shell holes just broaden and shift the lines and it is not possible to obtain in a direct way information about the M-shell ionization. It is obvious that the O-induced K x-ray spectra are rather complicated and need therefore an elaborated analysis.

In order to obtain information about the M-shell ionization we propose a method for the analysis of the K x-ray spectra of multiply ionized medium-Z atoms, which are produced in near-central collisions with energetic heavy projectiles. In this method the measured $K\alpha$ and $K\beta$ lines are assumed to be linear combinations of all possible $K\alpha L^nM^m$ and $K\beta L^nM^m$ profiles. The latter are constructed theoretically using transition energies and transition probabilities determined by extensive MCDF calculations. Assuming a binomial distribution of holes in the M shell and treating the M-shell ionization probabilities as adjustable parameters, the measured $K\alpha$ and $K\beta$ spectra are simultaneously decomposed into these theoretically constructed shapes.

A. MCDF calculations

The MCDF method employed in the present study has been described in detail in several papers [35,41–45]. Therefore, for the sake of clarity, only some essential ideas are briefly presented below. Within the MCDF scheme the effective Hamiltonian for an N-electron system is expressed by

$$H=\sum_{i=1}^{N} h_D(i)+\sum_{\substack{i,j\\ i=1\\ i<j}}^{N} C_{ij} \ , \tag{1}$$

where $h_D(i)$ is the Dirac operator for the ith electron and the terms C_{ij} account for electron-electron interactions. The latter are a sum of the Coulomb interaction operator and the transverse Breit operator. In this method the state function with the total angular momentum J and parity p is assumed to have the multiconfigurational form

$$\psi_s(J^p)=\sum_m c_m(s)\Phi(\gamma_m J^p) \ , \tag{2}$$

where $\Phi(\gamma_m J^p)$ are configuration-state functions (CSF), i.e., the antisymmetrized products of one-electron spinors, $c_m(s)$ are the configuration mixing coefficients for state s, and γ_m represents all the information needed to uniquely define a certain CSF.

There are several ways to perform MCDF calculations; in the optimal level (OL) version [35] the set of one-electron spinors and the set of CSF mixing coefficients are optimum for a particular state α: $E_{\rm opt}=E_\alpha$. For multiply ionized heavy atoms the x-ray transitions occur between hundreds of initial and final states so that the MCDF-OL calculations require a great amount of computer time. Another difficulty arises from the nonorthogonality of the orbitals corresponding to pairs of initial

and final states in the calculation of the transition probabilities. Therefore the versions of the MCDF method, which use a common set of orbitals for all the initial and final states are a good alternative. In the standard average-level scheme of MCDF calculations [35] $E_{\rm opt}$ is taken in the form

$$E_{\rm opt}=\frac{1}{n}\sum_{l=1}^{n}H_{ll}\ , \tag{3}$$

where n is the total number of CSF's (initial and final) and H_{ll} are the diagonal elements of the Hamiltonian matrix. This removes the problem of the nonorthogonality of the orbitals. However, the definition of $E_{\rm opt}$ in Eq. (3) does not consider the different numbers of initial and final states, but favors those states (initial or final) which are more numerous. Therefore, it was proposed [34] in the special average-level version of MCDF calculations to make use of an energy functional which gives a compensation of this imbalance.

An even better agreement with experimental diagram (see Table I) and satellite (see Ref. [2]) x-ray energies is obtained by using the recently proposed functional in the modified special average-level (MSAL) version [47] of MCDF,

$$E_{\rm opt}=\frac{1}{\lambda+1}\left[\frac{\lambda}{n_i}\sum_{i=1}^{n_i}H_{ii}+\frac{1}{n_f}\sum_{f=1}^{n_f}H_{ff}\right]\ , \tag{4}$$

where n_i and n_f are the numbers of initial and final states, H_{ii} and H_{ff} are the diagonal elements of the Hamiltonian matrix, and λ is a factor which depends on the K x-ray transition: $\lambda_{K\alpha}=0.5$, $\lambda_{K\beta_{1,3}}=0.65$, and $\lambda_{K\beta_2}=0.8$.

In the present study we used the computer program package GRASP [48], which allows relativistic MCDF calculations with the inclusion of the transverse (Breit) interaction and QED (self-energy and vacuum-polarization) corrections.

B. Couplings and shifts

The multiple initial and final states leading to a single L^nM^m satellite line are caused by a coupling of the open subshells. In the code GRASP the *jj* coupling scheme is applied. Assuming full outer subshells, for $K\alpha L^0M^0$ transitions there is only one initial state but two final states, leading to the $K\alpha_1$ and $K\alpha_2$ transitions. With one additional vacancy in the L shell a coupling between K and L shell is possible and the initial state consists of six different states. If the K hole is filled by an electron from the L shell the two L-shell holes can form nine states. Between these initial and final states 20 transitions of the type $K\alpha L^1$ are allowed. If the K hole is filled by an elec-

TABLE I. Calculated and standard (Ref. [46]) K x-ray energies in eV for Mo. $E_{4d^55s^1}$ was calculated with the experimental electron configuration $4s^24p^64d^55s^1$ and $E_{4d^45s^2}$ with the configuration $4s^24p^64d^4_{3/2}4d^0_{5/2}5s^2$ (see text).

Transition	$E_{4d^55s^1}$	$E_{4d^45s^2}$	$E_{\rm Bearden}$
$K\alpha_1$	17 479.6	17 479.5	17 479.34(2)
$K\alpha_2$	17 374.8	17374.2	17 374.3(1)
$K\beta_1$	19 607.4	19 607.2	19 608.3(3)
$K\beta_3$	19 589.8	19 589.5	19 590.3(3)
$K\beta_2$	19 964.8	19 965.5	19 965.2(6)

TABLE II. Calculated average energy shift of the satellite transitions with respect to the diagram lines (in eV), total intensity per second (sum of products of transition probability times degeneracy of initial state), and number of transitions for different diagram and satellite K x-ray lines of Mo. The configuration $4s^24p^64d^4_{3/2}4d^0_{5/2}5s^2$ has been used for the ground state of Mo. The numbers in brackets denote a multiplicative power of ten.

X-ray line	Energy shift	Intensity	Number
$K\alpha_1L^0M^0$		5.637[15]	1
$K\alpha_1L^0M^1$	3.0	1.026[17]	42
$K\alpha_1L^0M^2$	5.1	8.735[17]	1'057
$K\alpha_1L^0M^3$	7.4	4.652[18]	15'722
$K\alpha_1L^0M^4$	10.2	1.754[19]	137'315
$K\alpha_2L^0M^0$		2.963[15]	1
$K\alpha_2L^0M^1$	2.2	5.378[16]	30
$K\alpha_2L^0M^2$	4.4	4.597[17]	640
$K\alpha_2L^0M^3$	6.5	2.461[18]	8'602
$K\alpha_2L^0M^4$	8.8	9.235[18]	75'338
$K\alpha_1L^1M^0$	53.8	4.143[16]	11
$K\alpha_1L^1M^1$	56.4	7.463[17]	589
$K\alpha_1L^1M^2$	59.8	6.408[18]	16 010
$K\alpha_2L^1M^0$	50.2	2.010[16]	9
$K\alpha_2L^1M^1$	52.5	3.617[17]	407
$K\alpha_2L^1M^2$	54.4	3.199[18]	10 528
$K\alpha_1L^2M^0$	110.3	1.266[17]	47
$K\alpha_2L^2M^0$	104.6	6.185[16]	37
$K\alpha_{1,2}L^3M^0$	166.9	3.207[17]	170
$K\beta_{1,3}L^0M^0$		1.423[15]	2
$K\beta_{1,3}L^0M^1$	13.1	2.458[16]	56
$K\beta_{1,3}L^0M^2$	27.2	1.999[17]	1'029
$K\beta_{1,3}L^0M^3$	42.2	1.011[18]	11'631
$K\beta_{1,3}L^0M^4$	58.0	1.219[18]	81'184
$K\beta_{1,3}L^1M^0$	119.4	1.219[16]	36
$K\beta_{1,3}L^1M^1$	136.0	2.043[17]	1'515
$K\beta_{1,3}L^1M^2$	148.7	1.658[18]	32'083
$K\beta_{1,3}L^2M^0$	241.1	4.398[16]	233
$K\beta_{1,3}L^3M^0$	364.7	9.186[16]	688
$K\beta_2L^0M^0$		2.598[14]	2
$K\beta_2L^0M^1$	30.7	2.292[15]	36
$K\beta_2L^0M^2$	62.7	4.568[16]	1'698
$K\beta_2L^1M^0$	146.8	2.292[15]	36
$K\beta_2L^1M^1$	179.2	4.381[16]	1'921
$K\beta_2L^1M^2$	212.5	3.985[17]	53'123
$K\beta_2L^2M^0$	296.9	8.811[15]	233

tron from the $M_{II,III}$ subshells, the coupling of the spectator L- and the M-shell hole gives 14 final states and 36 $K\beta_{1,3}L^1$ transitions. Adding more L- or M-shell holes increases the number of states and transitions enormously. Of course, many of these transitions have only weak probabilities and can be neglected. The transition energies are slightly different and are distributed around some average energy.

The magnitude of the energy splitting depends on the shells which are coupled. For example, a $2s_{1/2}$ and a $2p_{1/2}$ hole can build a $J=0$ and a $J=1$ state. The calculated energy difference of these two states is 21.3 eV. For a $2s_{1/2}$ and a $4p_{1/2}$ hole the difference is only 0.2 eV. These values have then to be compared with the natural width of the x rays (6.8 eV for $K\alpha_1$) and the instrumental resolution (6.5 eV for $K\alpha_1$). Most of the transitions are lying so close together that the individual components are not resolvable. The splitting caused by the coupling of N- or O-shell holes to K-, L-, or M-shell holes is small (much smaller than the natural width) and its influence on the shape of the x rays can be neglected.

Spectator vacancies produce not only a widening of the line shape, but also a shift of the average energy with respect to the diagram line. The latter is caused by the reduction of the screening of the nuclear charge. The shift depends on the shell and subshell of the spectator vacancy and on the type of the K x-ray transition. In Table I the calculated energies of the K diagram x-ray transitions are presented and Table II gives for different satellite lines the calculated average shifts with respect to the diagram line, the total intensities, and the number of transitions. Shifts due to L-shell holes are almost an order of magnitude bigger than shifts due to M-shell holes. N- or O-shell vacancies produce negligible shifts.

It is worth noting that not only the average shifts presented in Table II are of importance for our analysis, but also the different shifts due to distinct M-subshell holes. A hole in the $3s$ or $3p$ subshells, for example, shifts the Mo $K\beta_1$ transition energy by about 17 eV but a hole in the $3d$ subshells by 10 eV. The energies of the $K\alpha$ transitions with one additional $3s$ hole are shifted by about 4 eV, with one $3p$ hole by about 8 eV, whereas for a $3d$ hole small shifts towards lower energies of -1 eV are obtained. This fact is very important for the analysis of the spectra and will be shown later.

C. Details of analysis

The theoretical energies and probabilities of all transitions contributing to a particular KL^nM^m line were calculated by means of the MCDF-MSAL version [47] of the code GRASP [48]. The line shapes of these transitions were constructed by folding their Lorentzian natural line shape with the known Gaussian instrumental response, resulting in so-called Voigt profiles. The theoretical KL^nM^m x-ray line shape was then computed by summing up all these Voigt functions multiplied by their transition probabilities. Applying this method to all possible $K\alpha L^nM^m$ and $K\beta L^nM^m$ lines and assuming that the K spectra are linear combinations of the latter, we were able to reproduce the observed spectra.

In practice, to keep the problem tractable, some truncations have to be made. The experimental electron configuration [49] of the neutral Mo atom is $4s^24p^64d^55s^1$, i.e., Mo has in its ground state two open subshells, namely the $4d$ and the $5s$. If we remove one electron from the K shell, the three open subshells give rise to 144 configurations in the initial state and to 417 configurations in the final state of a K diagram transition. The $K\alpha$, $K\beta_{1,3}$, or $K\beta_2$ lines consist thus of 28 076 transitions. For example, for $K\alpha$ the most intensive transitions are concentrated in two very narrow groups corresponding to $K\alpha_1$ and $K\alpha_2$. Such a calculation is very difficult and needs much computer time and memory space. Adding spectator vacancies makes the problem even much more complicated and in practice it is impossible to perform these calculations. Therefore, we have chosen for the neutral atom the configuration $4s^24p^64d^4_{3/2}4d^0_{5/2}5s^2$. The neutral atom has then only full or empty subshells and $K\alpha_1$ and $K\alpha_2$ consist of just one transition each. This artificial configuration produces a negligible energy shift (see Table I) and after convolution with the instrumental response, the change in the shapes of the K x-ray lines is insignificant.

Since with an increasing number of spectator vacancies the number of transitions increases very fast (see Table II) the calculation of K x-ray lines with multiple additional L- or M-shell holes becomes tedious. Thus, we decided to analyze with the above-described method only the $K\alpha L^0$ and the $K\beta_{1,3}L^0$ peaks to investigate the M-shell ionization and to take the shape of the $K\alpha L^nM^0$ and $K\beta L^nM^0$ peaks for the analysis of the L-shell ionization.

All $K\alpha L^0M^m$ and $K\beta_{1,3}L^0M^m$ transitions, where $0 \le m \le 4$, with all possible combinations of M-subshell holes were calculated. Figures 2 and 3 show these lines. It can be seen that the M^2, M^3, and M^4 satellites are shifted in energy, but the line shapes are not very

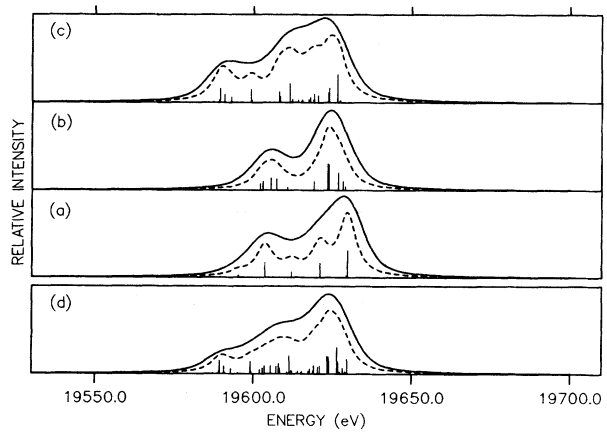

FIG. 2. Calculated $K\beta_{1,3}L^0M_i^1$ spectra of Mo with vacancies in the different subshells. Line positions and relative intensities (bars), Lorentzian natural line shapes (dashed line), and Voigt profiles after convolution with the instrumental line shape (solid line) are shown. The additional vacancy is in the (a) $3s$ subshell, (b) $3p$ subshells, (c) $3d$ subshells, (d) sum spectrum (a) plus (b) plus (c).

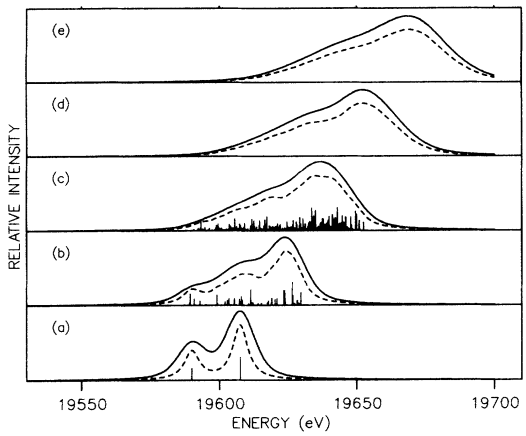

FIG. 3. Calculated $K\beta_{1,3}L^0M^m$ spectra of Mo. (For an explanation of the lines see Fig. 2.) (a) $K\beta_{1,3}L^0M^0$, (b) $K\beta_{1,3}L^0M^1$, (c) $K\beta_{1,3}L^0M^2$, (d) $K\beta_{1,3}L^0M^3$, (e) $K\beta_{1,3}L^0M^4$.

different. Thus the M^5, M^6, and M^7 satellites have been simulated by taking the line shapes of the M^4 satellites but shifted in energy. The energy shifts were determined as a combination of $(3sp)^m$ and $(3d)^m$, $5 \le m \le 7$, calculated shifts.

Assuming a binomial distribution (see Sec. IV) of the M-shell holes, the $K\alpha L^0$ and $K\beta_{1,3}L^0$ peaks were reproduced by fitting the theoretical $K\alpha L^0M^m$ and $K\beta_{1,3}L^0M^m$ lines to these peaks. The binomial distribution is governed by a single parameter p_M^X, which is the probability per M-shell electron to be ionized at the moment of the K x-ray transition. This parameter is common for all subshells and represents an average value. The L^1 satellites were taken into account in the fitting procedure as single peaks with larger Gaussian widths. The only free parameters in the fit were p_M^X, the background level, and an intensity scaling factor.

In a further step the analysis was performed by using two different probabilities: one, p_{3sp}^X, common for the $3s$ and $3p$ subshells, and the other, p_{3d}^X, for the $3d$ subshells.

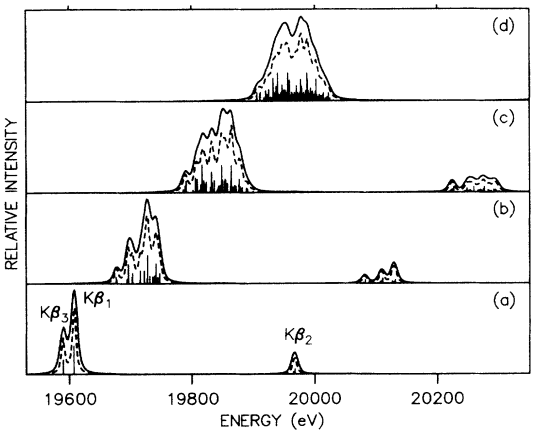

FIG. 4. Calculated $K\beta_{1,3}L^nM^0$ and $K\beta_2L^nM^0$ spectra of Mo. (For an explanation of the lines see Fig. 2.) (a) $K\beta L^0M^0$, (b) $K\beta L^1M^0$, (c) $K\beta L^2M^0$, (d) $K\beta L^3M^0$.

TABLE III. Fitted energy shifts (eV) of the measured $K\alpha L^n$ and $K\beta_{1,3}L^n$ lines with respect to the calculated $K\alpha L^nM^0$ and $K\beta_{1,3}L^nM^0$ profiles and fitted Gaussian widths (in eV) of the $K\beta_{1,3}L^n$ lines.

n	Energy shift $K\alpha L^n$	Energy shift $K\beta_{1,3}L^n$	Gaussian width
0	7.0±0.3	48.4±0.7	69.8±1.8
1	8.0±0.4	50.2±0.8	67.2±2.7
2	9.4±0.7	51.8±1.5	74.8±5.1

Assuming again binomial distributions for the M-subshell holes the $K\alpha L^0(3sp)^{m_1}(3d)^{m_2}$ and $K\beta_{1,3}L^0(3sp)^{m_1}(3d)^{m_2}$ lines were fitted to the measured spectra and the two probabilities p_{3sp}^X and p_{3d}^X could be determined.

In the analysis of the L satellites on the basis of the calculated $K\alpha L^nM^0$ and $K\beta L^nM^0$ lines (see Fig. 4) the effect of M-shell holes has to be taken into account, since the latter produce a shift of the center of gravity of the lines and a widening of the peaks. The widening can be simulated by taking a larger Gaussian width for the convolution with the Lorentzian curve. The calculated $K\alpha L^{0-3}$, $K\beta_{1,3}L^{0-3}$, and $K\beta_2L^{0-2}$ lines were fitted to the experimental spectra. For the $K\beta_{1,3}L^{0-2}$ lines, energy shifts, Gaussian widths, and peak intensities were left as free parameters. Table III shows the fitted values of the energy shifts and Gaussian widths of these three peaks. For $K\beta_{1,3}L^3$ the energy shift and the Gaussian width had to be fixed (corresponding to the values of $K\beta_{1,3}L^2$) and only the intensity was fitted. Since no significant structure appears in the $K\beta_2$ region, energy shifts and enlarged Gaussian widths had also to be fixed. A shift of 110 eV which corresponds to about 3.5 M-shell holes and a Gaussian FWHM of 117.5 eV for the Gaussian were chosen. An identical procedure was applied to the $K\alpha$ spectrum, but only one free parameter for the Gaussian width, common for all L satellites, was used (FWHM equal to 26.5 eV).

IV. RESULTS AND DISCUSSION

A. M-shell ionization

The removal of target M-shell electrons in a collision of 5.5-MeV/amu O ions with Mo is mainly due to the direct Coulomb-ionization process. In this process electrons are excited by the Coulomb interaction from their bound states to the continuum. If the independent particle picture is assumed and the excitation occurs without any correlations, the multiple ionization can be expressed by a binomial distribution with the ionization probability per M-shell electron p_M as the parameter. Other ionizing processes may, however, contribute to the M-shell ionization and change this distribution. In particular two processes have to be considered: the capture of bound target M-shell electrons by the projectile and competing decay processes to the K x rays, as LMM Auger transitions. But the influence of both processes is small and the as-

sumption of a binomial distribution is in a first approximation justified. (For a discussion of the competitive processes, see Sec. IV A 2.)

The probability per target M-shell electron to be captured by a bare oxygen projectile of 5.5-MeV/amu energy in a near-central collision was estimated using an n-body classical-trajectory Monte Carlo code [50]. The obtained value p_M^{EC} is on the order of 2×10^{-3}. A comparison with the experimental value for the M-shell ionization at the moment of the x-ray transition (see Sec. IV A 1) shows that in our case the capture process can be neglected. A confirmation of the minor role of electron capture with respect to direct ionization can be deduced from the results presented in Fig. 5. In this figure the ratios of experimental to theoretical (only direct Coulomb ionization) L- and M-shell ionization probabilities for the collisions of He and O projectiles with medium-Z target elements are plotted as a function of the reduced velocity $\eta=v_p/v_e$ (v_p is the projectile velocity and v_e the L- or M-shell electron velocity). For He projectiles the experimental L-shell ionization probabilities are not very different from the calculated ones, whereas for the M-shell ionization probabilities the difference is striking. A calculation shows that for He projectiles the cross section for electron capture and other ionizing processes is very small compared to the one for direct ionization [2]. The observed discrepancies were attributed to the use of hydrogenic electron wave functions [2,31]. For the L-shell ionization the ratios are much higher for collisions with O than with He ions, whereas for the M shell they are about equal. This indicates that for the L-shell ionization by O ions other ionizing processes are of importance, whereas for the M shell this is not the case. The most probable process to consider is electron capture [27].

Deviations from the independent-particle picture may be understood as electron correlation [51,52]. The shake-up and shake-off of electrons is such a correlation process. The ionization of the K shell causes a sudden change of the central potential acting on the target electrons. Due to that change, electrons can be promoted to higher shells or into the continuum. Carlson and Nestor [53] calculated electron shake-off probabilities as the result of x-ray photoionization of rare gases. Their results are applicable to any process that leads to a sudden creation of a vacancy in an atom. By creating a sudden vacancy in the K shell, we can estimate for Mo a shake-off probability of about $p_M^{shake}=2\times10^{-3}$. This value is much smaller than the value describing the M-shell ionization at the moment of the x-ray transition (see Sec. IV A 1).

1. Average M-shell ionization at the moment of the K x-ray emission

The p_M^X value determined from the fit of the $K\beta_{1,3}L^0$ peak is $p_M^X(K\beta_{1,3})=0.20$. For the determination of this parameter from the $K\alpha$ spectrum it is advantageous to consider the $K\alpha_2L^0$ line only because of an overlap of the intensities of the $K\alpha_1L^0$ peak and of the $K\alpha_2L^2$ satellite. The fit gives $p_M^X(K\alpha_2)=0.15$. Since the shift of the $K\alpha$ transitions due to the removal of $3d$ electrons is very small (see Sec. III B), the value of p_M^X determined from the $K\alpha$ spectrum is less reliable than from the $K\beta$ spectrum. A simultaneous fit of $K\alpha_2L^0$ and $K\beta_{1,3}L^0$ has also been performed. The resulting ionization probability is in good agreement with the value obtained by fitting the $K\beta_{1,3}L^0$ line alone, i.e., $p_M^X=0.19\pm0.02$. This corresponds to an average number of M-shell holes of $m=3.5\pm0.4$. Figures 6(a) and 6(b) show the $K\alpha_2L^0$ and the $K\beta_{1,3}L^0$ lines in detail with their M-satellite components. As one can see, the measured L^0 lines are reproduced rather satisfactorily, but nevertheless the fitted curves seem to be slightly shifted ($K\alpha$ towards higher energies and $K\beta$ towards lower energies). These discrepancies can be attributed to not equal M-subshell

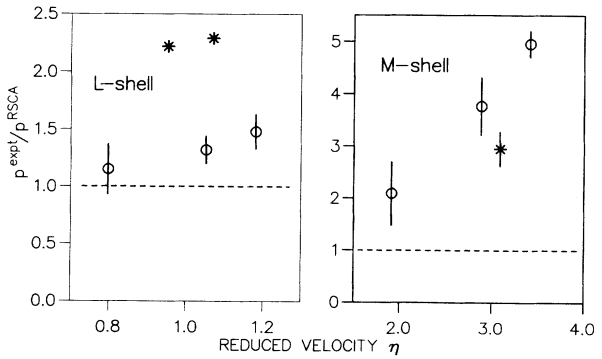

FIG. 5. Ratio of the experimental to the theoretical (RSCA) L- and M-shell ionization probability values plotted as a function of the reduced velocity. ○ denotes He-induced values: L shell (Ref. [31]), He (6.7 MeV/amu)+Mo, Pd, La; M shell (Ref. [2]), same as for L shell. * denotes O-induced values: L shell (Ref. [27]), O (5.5 MeV/amu)+Mo, Pd; M shell (this work), O (5.5 MeV/amu)+Mo.

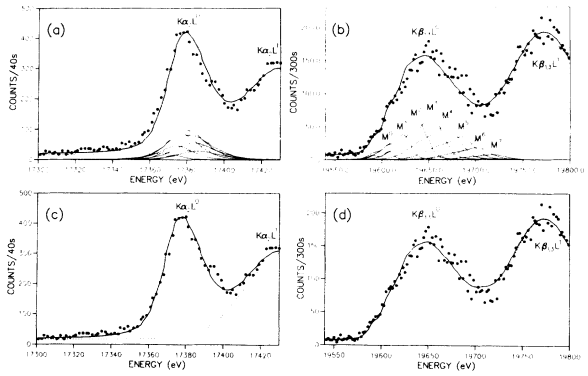

FIG. 6. (a) Fitted $K\alpha_2L^0$ line of Mo induced by 5.5 MeV/amu ^{16}O ions. One parameter p_M^X common for all M subshells is used. The solid lines represent the $K\alpha_2L^0M^m$ lines, the thick solid one the sum of them, and the dashed line the simulated L^1-satellite line. (b) Same as (a) but for the $K\beta_{1,3}L^0$ line. (c) Same as (a) but using two parameters p_{3sp}^X and p_{3d}^X, describing the unequal ionization of the M subshells. (d) Same as (c) but for the $K\beta_{1,3}L^0$ line.

ionization at the moment of the K x-ray transition (see Sec. IV B).

2. *Average M-shell ionization at the moment of the ion-atom collision*

The probability p_M^X reflects the number of holes in the M shell at the moment of the K x-ray transition. Although the decay of K holes occurs very fast, several competitive processes (the Auger, the Coster-Kronig, and radiative transitions for L and higher shells) may change the originally induced hole distribution. They can be accounted for by a statistical scaling procedure [54,27]. In our case, processes which produce one (*LLM* Coster-Kronig, *LMX* Auger, and radiative *L-M* transitions) and two (*LMM* Auger) M-shell holes and processes which fill up M-shell vacancies (*MXY* Auger and radiative M transitions) are important. Note that the *MMX* Coster-Kronig transitions change the distribution between the subshells, but not the total number of M holes.

The probability that an alternative transition takes place before the K-shell vacancy is filled is given by

$$R_{\text{alt}}=\frac{\Gamma_{\text{alt}}}{\Gamma_{\text{alt}}+\Gamma_K}\ , \tag{5}$$

where Γ_K is the K-shell width and Γ_{alt} the width of the alternative transition. Calculated transition probabilities for singly ionized atoms are known [55–61]. In a first-order approximation, for multiply ionized atoms the width of a transition is proportional to the number of electrons which can undergo the transition and to the number of holes in a subshell which can be filled.

All processes producing one or two additional M-shell holes need in the initial state one hole in the L shell. Therefore, only a part of them given by

$$\alpha=\frac{I(L^1)}{I(L^1)+I(L^0)}=0.57 \tag{6}$$

can contribute to the production of M-shell holes (see Sec. IV D). $I(L^0)$ and $I(L^1)$ are the intensities of the L^0 and L^1 satellite transitions, respectively. The absolute number of additional holes m_+ is then

$$m_+=\sum q_{\text{alt}}\alpha R_{\text{alt}}=0.32\ , \tag{7}$$

where q_{alt} is the number of M-shell holes produced by a particular alternative process.

Among the processes which contribute to the filling up of the M-shell vacancies, the radiative M transitions can be neglected. The transition probabilities of the *MXY* Auger transitions have to be multiplied by a factor of about 3.5, since in the initial state the atom has not only one but about 3.5 M-shell holes, so that $m_-=0.09$ M-shell holes disappear by this process before the K x ray takes place. Taking into account these corrections the ionization probability per M-shell electron at the moment of the ion-atom collision is $p_M=0.18\pm0.02$.

B. *M*-subshell ionization

Different M-subshell ionization probabilities and rearrangement processes may give rise to unequally ionized M subshells at the moment of the K x-ray transition. Especially *MMX* Coster-Kronig transitions can transfer $3s$ or $3p$ holes into $3d$ holes. To take into consideration the possibility of unequal M-subshell ionization, a second step in the analysis was performed, in which the single ionization probability parameter p_M^X was replaced by two free parameters, p_{3sp}^X and p_{3d}^X, the ionization probabilities for the $3s$ and $3p$ subshells and for the $3d$ ones, respectively. For their determination a simultaneous fit of the $K\alpha_2L^0$ and $K\beta_{1,3}L^0$ lines is essential, since two parameters have to be determined. The fit should not be carried out independently: for a fit of $K\alpha_2$ alone, for example, an absurd value for p_{3d}^X is obtained, because $3d$ holes produce only a very small negative shift. In a simultaneous fit of both lines, $K\alpha_2L^0$ is important for the determination of p_{3sp}^X, since the whole shift of the latter is due to $3s$ and $3p$ vacancies. In the same way $K\beta_{1,3}L^0$ is important for p_{3d}^X, because this parameter cannot be determined from $K\alpha$. Fitting $K\alpha_2$ and $K\beta_{1,3}$ simultaneously with two parameters it is possible to reproduce the experimental data much better [see Figs. 6(c) and 6(d)]. The obtained probabilities are $p_{3sp}^X=0.17\pm0.02$ and $p_{3d}^X=0.23\pm0.02$.

The weighted average of these two numbers is $p_{3spd}^X=0.205$. This shows that the value of p_M^X, which is about 6% smaller is also reasonable. The p_M^X value is slightly smaller, because by fitting with just one parameter the higher ionization of the $3d$ subshells at the moment of the K x-ray transition cannot be taken into account.

As mentioned above, the main difference in the ionization of the M subshells is caused by the $M_{sp}M_dX$ Coster-Kronig transitions. The probability that such a process occurs before the K x ray takes place is given by

$$\frac{\Gamma_{M_{sp}M_dX}}{\Gamma_{M_{sp}M_dX}+\Gamma_K}=\frac{2.1}{2.1+4.5}=0.32\ . \tag{8}$$

A necessary condition is that the initial state has at least one vacancy in the $3s$ or $3p$ subshells. Thus $\frac{8}{18}$ of all M-shell holes can contribute to this process so that 14% of all M holes change from the $3s$ or $3p$ subshells to the $3d$ subshells. Taking also into account that the *LLM* Coster-Kronig process produces only $3d$ holes, the expected subshell ionization probabilities at the moment of the x-ray transition were deduced from the measured average value p_M^X. They are p_{3sp}^X (theor)$=0.17$ and p_{3d}^X(theor)$=0.22$. This good agreement with the measured values suggests that differences between p_{3sp}^X and p_{3d}^X are mainly due to Coster-Kronig transitions, rather than to different subshell ionization probabilities at the moment of the collision.

C. Calculated SCA *M*-shell ionization probability

For the comparison of the ionization probabilities with theoretical calculations we have used the semiclassical

approximation [62], which is the only sufficiently developed theoretical model to allow a detailed comparison with impact-parameter-dependent probabilities. The measured M-shell ionization probability refers to a near-central collision since for a K transition an initial K-shell hole must be present and the M-shell ionization probability can be considered as constant over the whole impact-parameter range for which the K-shell ionization occurs.

Using the SCA version of Trautmann and Rösel [63,64] the calculations were performed with relativistic hydrogenic wave functions and a classical hyperbolic trajectory (RSCA). The screening effects were taken into account by introducing an effective charge according to the Slater rule. The calculations show that the differences in the M-subshell ionization probabilities for an impact parameter $b=500$ fm (for the choice of b see Ref. [2]) are negligibly small, which confirms our conclusion about the reasons for differences in the M-subshell ionization (see Sec. IV B). The average of the calculated values is p_M^{RSCA} (500 fm)$=$ 0.06. This value is three times smaller than the experimental one.

A similar disagreement was observed in measurements where He was the projectile (see Fig. 5 and Refs. [2] and [31]). The discrepancies were attributed to the improper approximations associated with the use of hydrogenic electron wave functions [2,31].

D. L-shell ionization

The fitted relative intensity yields X^n of the Mo $K\beta_{1,3}L^n$ lines are given in Table IV and the fitted Mo $K\beta$ spectrum is shown in Fig. 7. For the rearrangement correction the same procedure as in Ref. [27] has been used, but with the assumption that the widths are proportional to the number of vacancies located in the subshell which is filled by the electron undergoing the transition. The errors on the calculated radiative and nonradiative widths [58,60,61] have been assumed to be 10%. The corresponding primary vacancy yields are also shown in Table IV. Contrary to the M-shell ionization (see Sec. IV A 1), the rearrangement procedure shifts the mean value of L-shell hole number from 1.04 to a slightly higher value of 1.15.

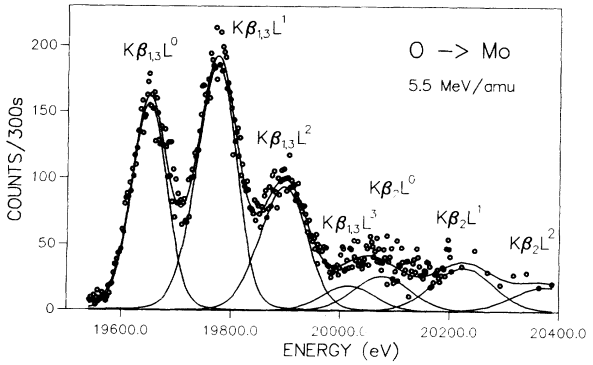

FIG. 7. Fitted Mo $K\beta$ spectrum induced by 5.5-MeV/amu ^{16}O ions. (The correction for the increased self-absorption for energies higher than the K edge is taken into account.)

TABLE IV. Relative x-ray intensity yields X^n and primary vacancy yields I^n deduced from the $K\alpha$ and $K\beta$ x-ray L-satellite intensities. X_R^n are the values from Ref. [27], where the L^n satellites were reproduced by just one Voigt function. The sum of the intensities is normalized to 1000.

n	$X^n(K\alpha)$	$X_R^n(K\alpha)$	$X^n(K\beta)$	$I^n(K\alpha)$	$I^n(K\beta)$
0	382(13)	373(7)	304(7)	293(19)	274(30)
1	403(18)	440(34)	403(9)	400(34)	388(42)
2	179(7)	160(19)	239(9)	222(22)	257(33)
3	37(4)	27(7)	54(8)	85(10)	84(16)

The experimental x-ray intensity ratio $X(K\beta_2L^0)$: $X(K\beta_2L^1)$: $X(K\beta_2L^2)$ is 100(10):135(11):80(17). It is in good agreement with the result obtained for the $K\beta_{1,3}$ lines. The ratio $X(K\beta_2L^0)$:$X(K\beta_{1,3}L^0)=0.26(2)$ can be compared with the corresponding ratio obtained from the He-induced measurements, which have been performed with the same experimental setup, i.e., $X(K\beta_2L^0)^{\mathrm{He}}$:$X(K\beta_{1,3}L^0)^{\mathrm{He}}=0.17(1)$. The difference is mainly due to the much stronger M-shell ionization in the O-induced spectrum, which diminishes the relative intensity of the $K\beta_{1,3}$ transitions. It should be noted that the ratios have not been corrected for the energy-dependent efficiency of the spectrum.

Using the calculated $K\alpha L^nM^0$ satellite structure, the $K\alpha$ spectrum has been reanalyzed. The results are also given in Table IV together with the values of Rymuza *et al.* [27]. In this previous work the satellites were fitted with just one line with a larger Gaussian width. Compared to the theoretical $K\beta_{1,3}L^n$ yields, the satellite intensities from the new fit are smaller. Since $2p$ electrons are responsible for a $K\alpha$ transition, additional L-shell holes reduce the $K\alpha$ transition intensity. Therefore, the yields corrected for rearrangement processes and fluorescence yields and not the x-ray yields have to be compared. The mean value of the L-shell hole number is shifted by the rearrangement procedure from 0.87 to 1.10.

The analysis of the $K\beta_{1,3}L^n$ lines evinces that the degree of M-shell ionization is the same for the $n=0$, 1, and 2 lines. Table III shows that the energy shifts and the Gaussian widths are almost identical. This justifies the choice of fixed values for these parameters for the $K\beta_{1,3}L^n$ and for the $K\beta_2L^n$ lines.

V. SUMMARY AND CONCLUSIONS

The principal aim of the present study was to extend our knowledge on the ionization process in near-central collisions of energetic heavy ions with medium-Z atoms. High-resolution measurements of O-induced K x-ray spectra of molybdenum were performed. Since in heavy-ion–atom collisions multiple ionization of the M and L shells of the target atom is very likely to occur, the structure of the observed spectra is very complex. In order to obtain information about the M-shell ionization in such a collision, an alternative method is proposed. In this method the measured $K\alpha$ and $K\beta$ spectra are simultaneously decomposed into theoretically constructed profiles

for all $K\alpha L^n M^m$ and $K\beta L^n M^m$ transitions, assuming a binomial distribution of holes in the M shell and treating the M-shell ionization probabilities as adjustable parameters. The average number of M-shell holes at the moment of the K x-ray transition has been determined to be $m=3.5\pm0.4$, corresponding to $p_M^X=0.19\pm0.02$. Taking into account the effect of rearrangement processes the ionization probability at the moment of the collision is $p_M=0.18\pm0.02$. For comparison the theoretical (RSCA) value is $p_M^{\mathrm{RSCA}}=0.06$. The ionization of the $3s$ or $3p$ and $3d$ subshells was determined to be $p_{3sp}^X=0.17\pm0.02$ and $p_{3d}^X=0.23\pm0.02$.

The spectra were also analyzed with respect to the L-shell ionization on the basis of the calculated $K\alpha L^0 M^0$, $K\beta_{1,3} L^n M^0$, and $K\beta_2 L^n M^0$ lines. The additional M-shell ionization was taken into account by using a larger Gaussian width and shifting the positions of the lines. The intensity yields of the L satellites were determined and the primary vacancy distribution was deduced. The analysis of the $K\alpha$ and $K\beta$ spectra gives an average number of L-shell holes at the moment of the collision of $l=1.12$.

On the basis of the presented study some general conclusions can be drawn. First, reliable results can only be obtained by fitting simultaneously the $K\alpha$ and $K\beta$ spectra. Second, to obtain a good fit to both spectra it is not enough to use a common parameter for all the subshells, which describes the average M-shell ionization at the moment of the K x-ray transition. The use of two parameters, one common for the $3s$ and $3p$ subshells and the other for the $3d$ subshells, gives a much better fit. Third, the fact that the average value of these two parameters is only slightly larger than p_M^X shows that, although the fit with one parameter is not very good, the p_M^X value is reasonable. Fourth, the differences in the M-subshell ionization at the moment of the K x-ray transition are mainly due to Coster-Kronig transitions, rather than to a different probability of the subshell ionization at the moment of the collision. Fifth, the discrepancy between our results deduced from the analysis of K x-ray spectra and the theoretical SCA values is attributed to the use of screened hydrogenic wave functions in the calculations. Sixth, in the case of L-shell ionization the rearrangement processes are much more important than in the case of the M-shell ionization (due to the importance of L Auger transitions). Only if they are taken into account, the vacancy distributions deduced from the $K\alpha$ spectrum and from the $K\beta$ spectrum are similar.

The authors do believe that the results of this study enable a deeper insight in the near-central collision processes and will stimulate a development of theoretical methods for the determination of ionization cross sections. The present study is a part of a broader project consisting of experiments with the aim of studying the multiple ionization induced in medium-Z atoms by heavy ions.

ACKNOWLEDGMENTS

This work was supported in part by the Swiss National Science Foundation and by the Paul Scherrer Institut (PSI) (formerly SIN). The authors are grateful to Dr. Stammbach and Dr. Schmelzbach and the cyclotron crew for good beam conditions. They would like to thank Professor D. Trautmann for making his program available for performing the calculations of the ionization probabilities and Dr. H. Aebischer for helpful discussions. One of us (M.P.) would like to thank the Swiss National Science Foundation for financial support and the Physics Department, University of Fribourg for its hospitality during his stay in Fribourg.

*Permanent address: Institute of Chemistry, Nicholas Copernicus University, 87-100 Toruń, Poland.

†Present address: GSI, Postfach 110541, D-6100 Darmstadt, Germany.

[1] M. Carlen, J.-Cl. Dousse, M. Gasser, J. Kern, Ch. Rhême, P. Rymuza, Z. Sujkowski, and D. Trautmann, Europhys. Lett. **13**, 231 (1990).

[2] M. Carlen, J.-Cl. Dousse, M. Gasser, J. Hoszowska, J. Kern, Ch. Rhême, P. Rymuza, Z. Sujkowski, and D. Trautmann, Z. Phys. D **23**, 71 (1992).

[3] P. Richard, in *Atomic Inner-Shell Processes*, edited by B. Crasemann (Academic, New York, 1975), Chap. 2, and references therein.

[4] F. Hopkins, in *Methods of Experimental Physics*, edited by P. Richard (Academic, New York, 1980), Vol. 17, Chap. 8, and references therein.

[5] P. Richard, I. L. Morgan, T. Furuta, and D. Burch, Phys. Rev. Lett. **23**, 1009 (1969).

[6] A. R. Knudson, D. J. Nagel, P. G. Burkhalter, and K. L. Dunning, Phys. Rev. Lett. **26**, 1149 (1971).

[7] D. Burch, P. Richard, and R. L. Blake, Phys. Rev. Lett. **26**, 1355 (1971).

[8] D. G. McCrary and P. Richard, Phys. Rev. A **8**, 1249 (1972).

[9] C. F. Moore, M. Senglaub, B. Johnson, and P. Richard, Phys. Lett. **40A**, 107 (1972).

[10] R. L. Kauffman, J. H. McGuire, P. Richard, and C. F. Moore, Phys. Rev. A **8**, 1233 (1973).

[11] T. K. Li, R. L. Watson, and J. S. Hansen, Phys. Rev. A **8**, 1258 (1973).

[12] P. Richard, R. L. Kauffman, J. H. McGuire, C. F. Moore, and D. K. Olson, Phys. Rev. A **8**, 1369 (1973).

[13] J. McWherter, J. Bolger, C. F. Moore, and P. Richard, Z. Phys. **263**, 283 (1973).

[14] R. L. Watson, F. E. Jenson, and T. Chiao, Phys. Rev. A **10**, 1230 (1974).

[15] A. R. Knudson, P. G. Burkhalter, and D. J. Nagel, Phys. Rev. A **10**, 2118 (1974).

[16] R. L. Kauffman, C. W. Wood, K. A. Jamison, and P. Richard, Phys. Rev. A **11**, 872 (1975).

[17] K. W. Hill, B. L. Doyle, S. M. Shafroth, D. H. Madison, and R. D. Deslattes, Phys. Rev. A **13**, 1334 (1976).

[18] J. A. Demarest and R. L. Watson, Phys. Rev. A **17**, 1302 (1978).

[19] C. Schmiedekamp, B. L. Doyle, T. J. Gray, R. K. Gardner, K. A. Jamison, and P. Richard, Phys. Rev. A **18**,

1892 (1978).
[20] R. L. Watson, B. I. Sonobe, J. A. Demarest, and A. Langenberg, Phys. Rev. A **19**, 1529 (1979).
[21] T. Tonuma, Y. Awaya, T. Kambara, H. Kumagai, I. Kohno, and S. Özkök, Phys. Rev. A **20**, 989 (1979).
[22] R. L. Watson, J. R. White, A. Langenberg, R. A. Kenefick, and C. C. Bahr, Phys. Rev. A **22**, 582 (1980).
[23] S. Raman *et al.*, Nucl. Instrum. Methods B **3**, 100 (1984).
[24] Y. Awaya, T. Kambara, M. Kase, H. Shibata, H. Kumagai, K. Fujima, J. Urakawa, T. Matsuo, and J. Takahashi, Nucl. Instrum. Methods B **10/11**, 53 (1985).
[25] C. R. Vane, E. Källne, J. Källne, G. Morford, S. Raman, and M. S. Smith, Nucl. Instrum. Methods B **10/11**, 190 (1985).
[26] B. Perny, J.-Cl. Dousse, M. Gasser, J. Kern, Ch. Rhême, P. Rymuza, and Z. Sujkowski, Phys. Rev. A **36**, 2120 (1987).
[27] P. Rymuza, Z. Sujkowski, M. Carlen, J.-Cl. Dousse, J. Kern, B. Perny, and Ch. Rhême, Z. Phys. D **14**, 37 (1989).
[28] R. Salziger, G. L. Borchert, D. Gotta, O. W. B. Schult, D. H. Jakubassa-Amundsen, P. A. Amundsen, and K. Rashid, J. Phys. B **22**, 821 (1989).
[29] D. F. Anagnostopoulos, G. L. Borchert, D. Gotta, and K. Rashid, Z. Phys. D **18**, 139 (1991).
[30] T. Ludziejewski, J. Hoszowska, P. Rymuza, Z. Sujkowski, D. Anagnostopoulos, G. Borchert, M. Carlen, J.-Cl. Dousse, Ch. Rhême, and A. Drentje, Nucl. Instrum. Methods B **63**, 494 (1992).
[31] P. Rymuza, T. Ludziewjewski, Z. Sujkowski, M. Carlen, J.-Cl. Dousse, M. Gasser, J. Kern, and Ch. Rhême, Z. Phys. D **23**, 81 (1992).
[32] M. Polasik, Phys. Rev. A **39**, 616 (1989).
[33] M. Polasik, Phys. Rev. A **39**, 5092 (1989).
[34] M. Polasik, Phys. Rev. A **40**, 4361 (1989).
[35] I. P. Grant, B. J. McKenzie, P. H. Norrington, D. F. Mayers, and N. C. Pyper, Comput. Phys. Commun. **21**, 207 (1980).
[36] B. Perny, J. Cl. Dousse, M. Gasser, J. Kern, R. Lanners, Ch. Rhême, and W. Schwitz, Nucl. Instrum. Methods A **267**, 120 (1988).
[37] J.-Cl. Dousse and J. Kern, Acta Crystallogr. Sect. A **36**, 966 (1980).
[38] S. I. Salem and P. L. Lee, At. Data Nucl. Data Tables **18**, 233 (1976).
[39] B. Jeckelmann *et al.*, Nucl. Instrum. Methods A **241**, 191 (1985).
[40] K. D. Sevier, At. Data Nucl. Data Tables **24**, 323 (1979).
[41] B. J. McKenzie, I. P. Grant, and P. H. Norrington, Comput. Phys. Commun. **21**, 233 (1980).
[42] I. P. Grant and B. J. McKenzie, J. Phys. B **13**, 2671 (1980).
[43] J. Hata and I. P. Grant, J. Phys. B **16**, 3713 (1983).
[44] I. P. Grant, Int. J. Quantum Chem. **25**, 23 (1984).
[45] I. P. Grant, J. Phys. B **7**, 1458 (1974).
[46] J. A. Bearden, Rev. Mod. Phys. **39**, 78 (1967).
[47] M. Polasik *et al.* (unpublished).
[48] K. G. Dyall, I. P. Grant, C. T. Johnson, F. A. Parpia, and E. P. Plummer, Comput. Phys. Commun. **55**, 425 (1989).
[49] *American Institute of Physics Handbook*, 3rd ed., edited by D. E. Gray (McGraw-Hill, New York, 1972), pp. 7–10.
[50] R. I. Olson, in *Electronic and Atomic Collisions*, edited by H. B. Gilbody, W. R. Newell, F. H. Read, and A. C. H. Smith (Elsevier, New York, 1988), p. 271.
[51] N. Stolterfoht, Phys. Scr. **42**, 192 (1990).
[52] J. O. P. Pedersen, Phys. Scr. **42**, 180 (1990).
[53] T. A. Carlson and C. W. Nestor, Phys. Rev. A **8**, 2887 (1973).
[54] F. P. Larkins, J. Phys. B **4**, L29 (1971).
[55] E. J. McGuire, Phys. Rev. A **3**, 587 (1971).
[56] E. J. McGuire, Phys. Rev. A **5**, 1043 (1972); **5**, 1052 (1972).
[57] J. H. Scofield, At. Data Nucl. Data Tables **14**, 121 (1974).
[58] O. Keski-Rahkonen and M. O. Krause, At. Data Nucl. Data Tables **14**, 139 (1974).
[59] M. H. Chen, B. Crasemann, and H. Mark, At. Data Nucl. Data Tables **24**, 13 (1979).
[60] M. H. Chen, B. Crasemann, and H. Mark, Phys. Rev. A **21**, 436 (1980).
[61] M. H. Chen, B. Crasemann, and H. Mark, Phys. Rev. A **24**, 177 (1981).
[62] J. Bang and J. M. Hansteen, Kgl. Dan. Vid. Selsk. Mat.—Fys. Medd. **31**, No. 13 (1959).
[63] D. Trautmann and F. Rösel, Nucl. Instrum. Methods **169**, 259 (1980).
[64] D. Trautmann, F. Rösel, and G. Baur, Nucl. Instrum. Methods **214**, 21 (1983).